Intelligent PI Controller and Its Application to Dissolved Oxygen Tracking Problem

Tomasz Zubowicz, Mieczysław A. Brdys, Robert Piotrowski

Abstract:

The paper addresses design, calibration, implementation and simulation of the intelligent PI controller used for dissolved oxygen (DO) tracking at wastewater treatment plant (WWTP). The calibration process presented in this paper utilizes both engineering and scientific methods. Verification of the control system design method was obtained via simulation experiments.

Keywords: *aeration process, artificial intelligence, control systems, dissolved oxygen, tracking problem, fuzzy logic controller, genetic algorithms, intelligent control, Takagi Sugeno Kang method, TSK, soft switching, wastewater treatment.*

1. Introduction

Control algorithms for the WWTP have been investigated intensively, particularly for DO control. The DO dynamics is nonlinear and of high dimension. Dissolved oxygen is the most important control parameter for biological processes in WWTP. Increasing performance of the DO control system is a basic action leading to improve the effectiveness and efficiency of the regarded system. It becomes more interesting when it can be done without interference into the system structure and only by simple manipulation of the control algorithm. The DO tracking problem is one of the most complex and still fundamental issue of biological WWTP involving activated sludge technology due to its influence on dynamics of biochemical processes. Its complexity derives from strong no linearity and time dependence of the process variables.

In this paper a very effective controller design approach is presented, which uses both classical and artificial intelligence methods to find a solution dissolved oxygen-tracking problem.

The paper is organized as follows. The problem statement is described in Section 2. Section 3 presents the PI controller design. The controller calibration process is described in Section 4. The engineering and scientific methods are used. Application of the controller to Kartuzy WWTP is described in Section 5 and the simulation results are presented. Section 6 concludes the paper.

2. Problem statement

The previous papers [Brdys, *et. al.*, 2002; Piotrowski, *et. al.*, 2004; Piotrowski, *et. al.*, 2008] propose a two level controller to track prescribed dissolved oxygen trajectory. The upper level control unit prescribes trajectories of desired airflows to be delivered into the aerobic biological reactor zones. The lower level controller forces the aeration system to follow these set point trajectories. A non-linear model predictive control algorithm is applied to design this controller unit.

The goal of this paper is to provide the design methodology of intelligent multiregional controller [Domanski, *et al.*, 1999], with enhanced regional controllers, to enable highly nonlinear system, in this case aeration system, to work in a whole control space with the same high quality performance under heavy disturbances. It also shows how to utilize optimization method to calibrate the resulting controller parameters.

Activated sludge wastewater treatment plant (ASWTP) is a very complex and demanding structure for closed-loop control due to its internal processes nonlinearities, inconsistency, and time and parameter variability. The scheme of the biological WWTP is presented in Fig. 1.

The advanced biological processes with nutrient removal is accomplished in the activated sludge reactor designed and operated according the University of Cape Town (UCT) process.

The first zone where the phosphorus is released is anaerobic.

The second zone where the denitrification process is conducted is anoxic.

The internal recirculation 2 of mixed liquor originates from the anoxic zone. The returned activated sludge from the bottom of the clarifiers and the internal recirculation 1 from the end of the aerobic zone (containing nitrates) are directed to the anoxic zone.
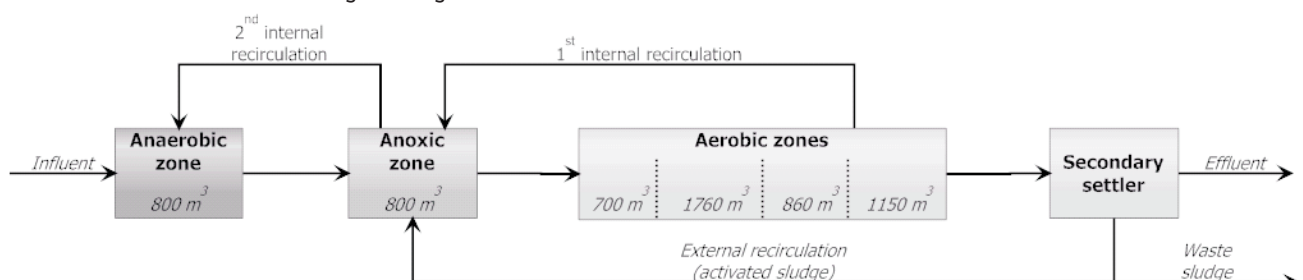

Fig. 1. Scheme of the biological WWTP.

The last part of the reactor (aerobic) is aerated by a diffused aeration system. This zone is divided into four compartments of various intensity of aeration.

The biologically treated wastewater and biomass (activated sludge) are separated in two parallel horizontal (rectangular) secondary clarifiers.

In order to ensure a high level of phosphorus removal, iron sulphate (PIX) is added to the aerobic zone to precipitate most of the remaining soluble phosphorus (simultaneous precipitation). There is also the opportunity to precipitate phosphorus in the grit chamber (pre-precipitation).

The excess biological sludge is stored in a thickener, then dewatered in two centrifuges and finally chemically stabilized in lime. It is expected that the sludge will be disposed of for agricultural applications.

For the purpose of the research the activated sludge model type ASM2d [Henze, *et al.*, 1995] was used. This selection was a good compromise between accuracy and speed in predicting dynamics of the biochemical processes [Brdys, *et al.*, 2004].

The ASM2d type model derives from the activated sludge model family (ASM), which also consists of the types ASM1, ASM2, ASM3, ASM3 Bio-P. The differences between each model are generally situated in their mathematical representation accuracy of biochemical processes. The ASM family evolved according to the stated order with ASM2d model placed in between ASM2 and ASM3.

The WWTP model was designed using commercial package Simba [Simba, 2005]. After the quality and quantity parameter identification the model calibration process was applied. For the purpose of calibration the genetic algorithms (GA) were used. Final step, the validation process verified and confirmed the usefulness of the constructed model.

3. Controller design

This section addresses directly the DO tracking problem. In [Yoo, *et al.*, 2002] for the purpose of solving the DO tracking problem the PI controller with on-line parameter adaptation was proposed. First of the mechanisms was invoked to enable in the controller ability to reject disturbances and the second to carry out control of the nonlinear process with the same performance in whole control area.

In this paper the more effective (regarding both controller design methodology and computational requirements) method was proposed. For the purpose of disturbance rejection the classical PI regulator was applied regionally. In order to enhance the regional fixed parameter controllers to work as a one in whole control space the control signal switching system was utilized. Due to decreasing of performance during the hard switching techniques, the artificial intelligence (AI)Takagi-Sugeno-Kangs (TSK) soft switching method is used (Fig. 2). This also has allowed to eliminate troubling parameter adaptation procedure presented in [Yoo, *et al.*, 2002].

For the purpose of the design process the following assumptions have been made:
- the aeration system is regarded as ideal thus the generated and reference airflows fulfill the expression:

$$Q_{air}(k) \equiv Q_{air}^{ref}(k);$$

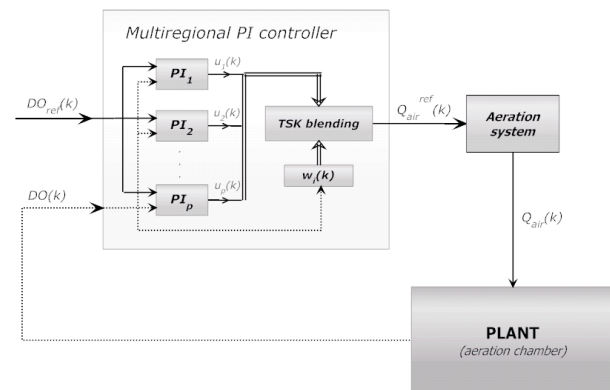- plant being under control is a single aeration chamber.

Fig. 2. Scheme of the control system.

The intelligent controller (Fig. 2) design process can be easily divided into four main stages:
- stage I gathering information;
- stage II region indication;
- stage III local controller design;
- stage IV fuzzy logic applying;
- stage V calibration (optional).

Stage I:

The first step that needs to be taken is to represent knowledge of the process in the form of static characteristic of DO as a function of airflow Q_{air}, generated by the aeration system. As mentioned before (see Section 2) the considered process is under heavy influence of time varying disturbances: wastewater inflow (Q), chemical oxygen demand (COD), total nitrogen (TN) and total phosphorus (TP). The model based sensitivity analysis per-formed to acquire the steady state characteristic of the process resulted in obtaining the whole family of $DO(Q_{air})$ curves. In Fig. 3, the mean $DO(Q_{air})$ characteristic (determined via the studies) and its boundaries have been shown.

Stage II:

As determined in Stage I the relationship between DO and Q_{air} is highly nonlinear (Fig 3). In the second stage the mean steady state characteristic is piecewise linearized (Fig. 4) for the purpose of nonlinearity approximation thus divided into affine, linear spaces (region indication: l_i, for $i = 1,..,5$). This method has many advantages such as: simplicity, ability to indicate linearly representative regions of process, associated error and above all in some cases can be done graphically (mainly while regarding SISO systems). This last feature enables the designer to decide if the balance between accuracy and complexity is maintained at proper level.

Piecewise linearization also can be done *via* an optimization algorithm with properly chosen cost function, but the first approach represents, in authors opinion, a good balance between simplicity and effectiveness and thus recommended for this and similar cases.
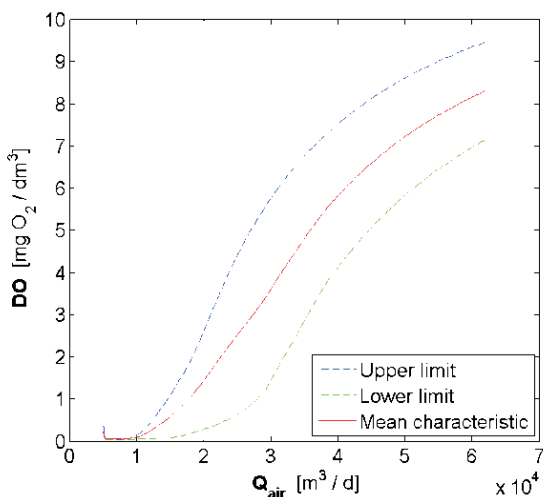
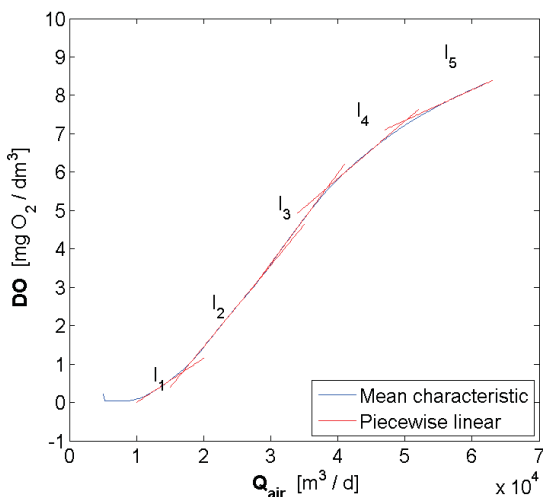Fig. 3. Static characteristic of the aeration process and its boundaries.

Fig. 4. Mean and piecewise linear static characteristic of the aeration process.

Stage III:

Indicating the regions with lack or small enough error, which can be treated as linear, allows looking for also linear regional controller.

PI controller is used for a local (regional) controller (Fig. 5). Additionally magnitude and rate limiter of the generated control signal have been added along with the anti wind-up filter controlling the performance of the magnitude limiter. As a result the nonlinear PI controller is used.

Incorporating stated nonlinearities into PI model results in many advantages. The magnitude and rate limiter enables controller to generate control signal meeting the actuator system static and dynamic limitations. Both influence the actuators lifespan and also time needed between maintenance by reducing stress generated in the system. The negative influence of saturation states entailed mostly by the magnitude limiter is reduced by the anti wind-up filter [Bohn and Atherton, 1995] utilized in the controller.

The PI controller (Fig. 5) can be described as:

$$
\begin{cases}
u(k) = g(k)(0.5 \cdot sat(u_p(k)) + 0.5) \\[2mm]
u_p(k) = 0.5 \cdot \displaystyle\sum_{i=1}^{p} sat(\Delta u_u(i)) \\[2mm]
u_u(k) = K_p e(k) + K_p K_i \displaystyle\sum_{j=1}^{p} u_i(j) \\[2mm]
u_i(k) = e(k) - K_{aw}(u_p(k) - 0.5 \cdot sat(u_p(k)) - 0.5
\end{cases}
\tag{1}
$$

where: $e(k)$ - error; $u(k)$ - control signal; $u_i(k)$ - signal in summation line; $u_{pre}(k)$ - signal before magnitude limitation; K_p - proportional gain; K_i - summation gain [1/s]; K_{aw} - anti wind-up filter gain; g - output scaling factor.

In the system (1) the error signal $e(k)$ is defined as:

$$
e(k) = \frac{1}{DO_{max}} (DO_{ref}(k) - DO(k))
\tag{2}
$$

where: $DO(k)$ - measured dissolved oxygen value; $DO_{ref}(k)$ - reference value of DO; DO_{max} - input scaling factor.

The saturation function is as follows:

$$
sat(.) = sign(.) min\{|.|, 1\}
\tag{3}
$$

The calibration of the local controllers parameters can simply be done using well-known engineering approach both *via* on plant experiments or model-based simulations. Parameters for the five local PI controllers (see Fig. 5) chosen arbitrary to balance the performance in each region have been presented in Table 1.
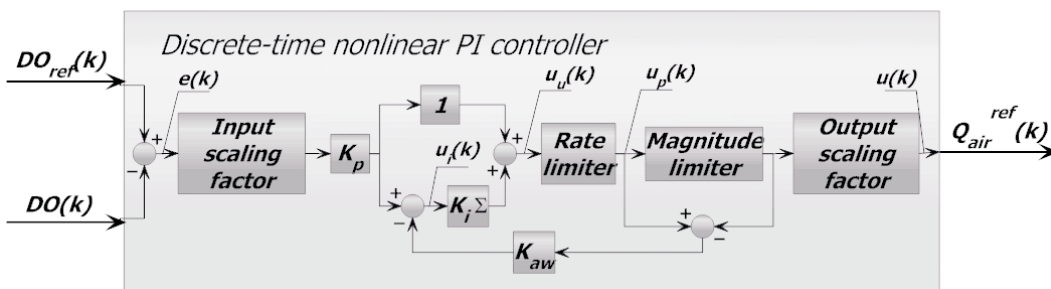

Fig. 5. Local discrete nonlinear PI controller.

Table 1. Values of local PI controller's parameters.

Name	Controller I	Controller II	Controller III	Controller IV	Controller V
Region	l_1	l_2	l_3	l_4	l_5
T_s [s]	30	30	30	30	30
$K_{i,i}$ [1/s]	0.04	0.02	0.01	0.03	0.02
$K_{p,i}$	16.83	10.54	6.44	14.98	11.29
$K_{aw,i}$	9.67	9.6	9.79	15.88	16.22

Stage IV

In this step the TSK fuzzy logic mechanism (4) is being applied [Yaochu, 2002; Tanaka and Sugeno, 1992]. The sole of the TSK can be seen as the weighted average (blended) control signals of regional controllers:

$$Q_{air}^{ref}(k) = \frac{\sum_{i=1}^{p} w_i(DO(k)) \cdot Q_{air,i}^{ref}(k)}{\sum_{i=1}^{p} w_i(DO(k))} \qquad (4)$$

where: $Q_{air}^{ref}(k)$ - multiregional controller output; $Q_{air,i}^{ref}(k)$ - output value of i-th regional controller; p - number of regions in this case $p = 5$.

The weights $w_i(DO)$ is on-line tuned according to the process state, which in this case is denoted by the DO concentration. The possible weight values are fuzzy sets of a priori defined membership functions (MFs). Each MF is directly correlated with corresponding regional controller; hence the number of regions determines the number of MFs. In this case the Sigmoidal and Gauss conditional functions were utilized [Yaochu, 2002].

Defining the MF simply means to chose its type and shape. It should be noted that the choice of the MFs is crucial for acquiring stability and good performance of the closed loop system, however it can be done while having basic knowledge of the process. It is also useful to know the shape of the assessed process static characteristic, which in this case is already achieved (see Stage I). The procedure for choosing MFs is as follows:
- each regional controller should be given a corresponding MF;
- the core of i-th MF should overlap with the part of i-th region that possesses relative error of approximation less then 10% (which is an arbitrary chosen value);
- the value of membership of i-th MF should be equal to 0 when it reaches the neighboring MFs core;
- created fuzzy partition should be normal and consistent.

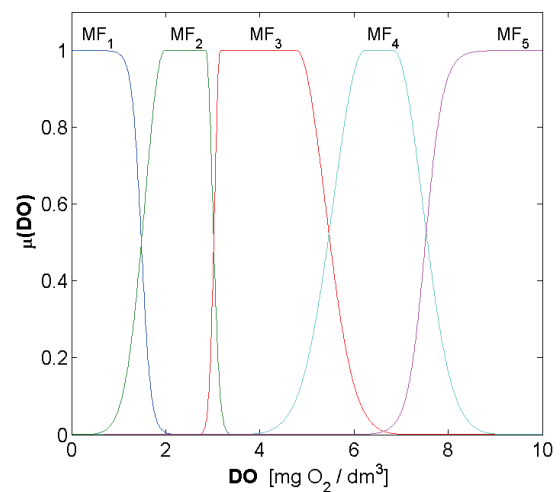Resulting fuzzy partition is presented in Fig. 6.

Fig. 6. Initial MFs.

The formulas for each MF and parameters in the numerical form have been presented in Table 2.

Stage V

Calibration of the MFs parameters is the final stage of the controller design process. This stage can be omitted with no loss of functionality of the designed control system, however it certainly improves the overall system performance. As a tool for that purpose the GA was chosen and applied. The whole calibration process is described in details in Section 4 due to its rather extensive character.

Table 2. MFs and their parameters.

No	Region	Function name	Formula	Parameters
1	l_1	Sigmoidal	$\mu_A(DO(k)) = \dfrac{1}{1+\exp(-a(DO(k)-c))}$	a = -10 c = 1.483
2	l_2	Gauss	$\mu_A(DO(k)) = \begin{cases} \exp\left[\dfrac{-(DO(k)-c_1)^2}{\sigma_1^2}\right]; \text{left - most curve} \\ 1; \quad\quad\quad\quad\quad \text{whenever } c_1 < c_2 \\ \exp\left[\dfrac{-(DO(k)-c_2)^2}{\sigma_2^2}\right]; \text{right - most curve} \end{cases}$	sig_1 = 0.422 c_1 = 1.98 sig_2 = 0.145 c_2 = 2.85

Table 2. MFs and their parameters.

No	Region	Function name	Formula	Parameters
3	l_3	Gauss		$sig_1 = 0.1146$ $c_1 = 3.155$ $sig_2 = 0.604$ $c_2 = 4.78$
4	l_4	Gauss		$sig_1 = 0.671$ $c_1 = 6.231$ $sig_2 = 0.612$ $c_2 = 6.84$
5	l_5	Sigmoidal	$\mu_A(DO(k)) = \dfrac{1}{1+\exp(-a(DO(k)-c))}$	$a = 5.38$ $c = 7.514$

4. MFs parameters calibration

4.1. Utilizing GA

In order to calibrate parameters of the MF, the GA was used due to their large number, task computational difficulty and lack of knowledge about system model derivatives.

The main features of the utilized algorithm are as follows [O'Reilly, *et al.*, 2002]:
- genes in a form of real numbers (16 genes see Table 2);
- initial population contains one fixed chromosome with genes equal to the parameters presented in Table 2;
- algorithm uses operands: mating (crossing and blending) and mutation both with gene value and duplicity control;
- elitism;
- generation counter as algorithm stop condition.

The cost function used to evaluate each chromosome is given by the formula:

$$JS = e^T Ee + M_\%^T M M_\% + \Delta M_\%^T \Delta M \Delta M_\% + t_R^T T_R t_R +$$
$$+ \Delta t_R^T \Delta T_R \Delta t_R + u^T Uu + \Delta u^T \Delta U \Delta u + aw^T Aaw +$$
$$+ du^T Ddu + n^T Nn + cm^T Ccm \qquad (5)$$

where: JS - survival cost; $e^T Ee$ - steady state error; $M_\%^T M_\%$ - percentage overshoot; $\Delta M_\%^T \Delta M \Delta M_\%$ - difference between overshoots within each region; $t_R^T T_R t_R$ - settling time with respect to 5% criterion; $\Delta t_R^T \Delta T_R \Delta t_R$ - difference between settling times within each region; $u^T Uu$ - control signal energy; $\Delta u^T \Delta U \Delta u$ - difference between regional control signals; $aw^T Aaw$ - saturation states; $du^T Ddu$ - oscillation in control signal; $n^T Nn$ - normality of fuzzy partitioning; $cm^T Ccm$ - consistency of fuzzy partitioning.

The algorithm flow chart is presented in Fig. 7, while the convergence of the GA over the generation is shown in Fig. 8.
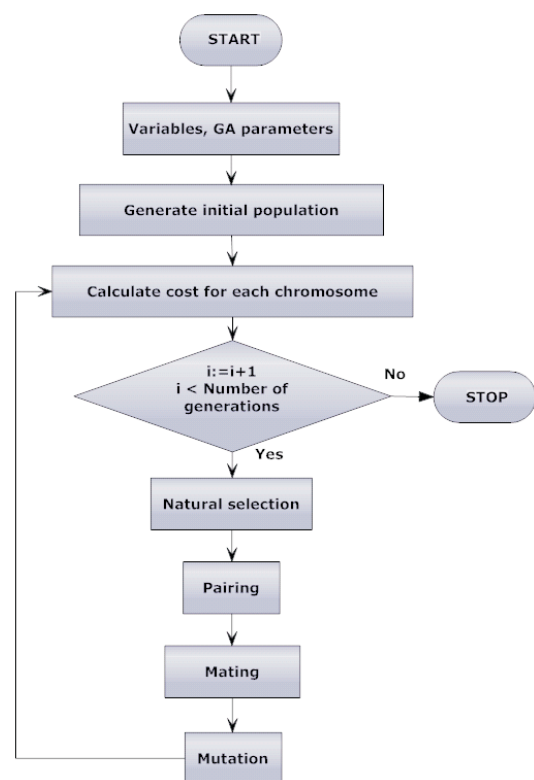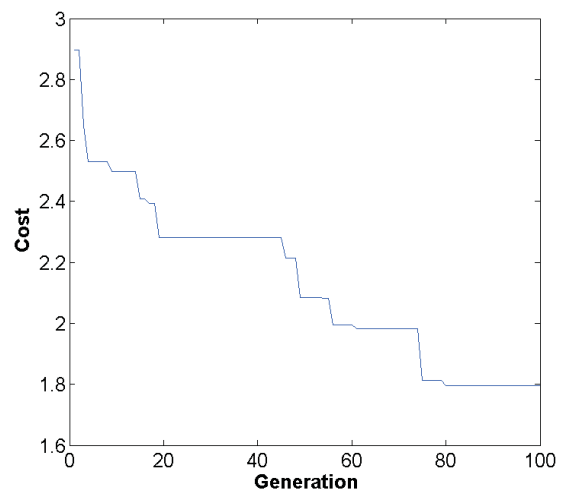

Fig. 7. GA flow chart.

Fig. 8. GA convergence.

Table 3. Calibrated MFs parameters.

Region	l_1	l_2	l_3	l_4	l_5
MF	MF_1	MF_2	MF_3	MF_4	MF_5
Parameters	a = -10.932	sig_1 = 0.371 c_1 = 1.868	sig_1 = 0.079 c_1 = 3.149	sig_1 = 0.412 c_1 = 6.311	a = 6.578
	c = 1.2052	sig_2 = 0.104 c_2 = 2.844	sig_2 = 0.427 c_2 = 5.049	sig_2 = 0.440 c_2 = 8.232	a = 6.578

Table 3 shows the last generation (100th) of the population, sorted in ascending order with regard to the cost.

The graphical representation of the functions is shown in Figure 9.
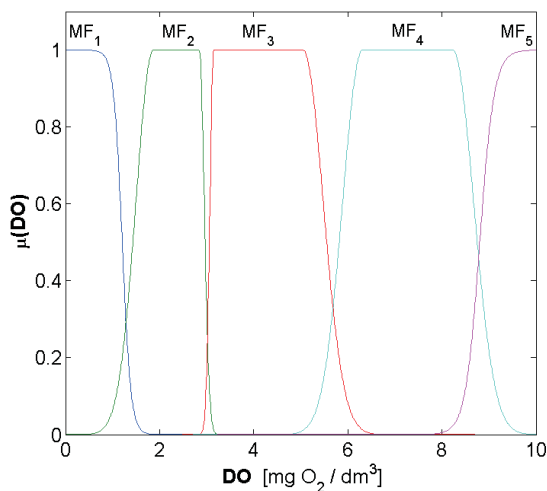
Fig. 9. MFs with calibrated parameters.

4.2. Calibration summary

The calibration process exploiting GA (in example [5]) makes this uneasy task achievable (see Fig. 8). In order to clearly show the differences in performance of MFs with and without calibration process a standard root mean square (RMS) criterion, given by (6) was used:

$$RMS = \sqrt{\frac{1}{N} \cdot J} \qquad (6)$$

where N is the number of samples and J is defined as follows (7):

$$J = e^T E e + M_\%^T M M_\% + \Delta M_\%^T \Delta M \Delta M_\% + t_R^T T_R t_R +$$

$$+ \Delta t_R^T \Delta T_R \Delta t_R + u^T U u + \Delta u^T \Delta U \Delta u + aw^T A aw \qquad (7)$$

The data collected have been presented in Table 4, along with the percentage value of performance enhancement (compared with the state before calibration).

As it can easily been seen examining the comparison results collected in the Table 4 the GA based approach increases the performance of the control system up to X% according to the RMS criterion.

5. Simulation results

In this section the derived controller is validated by simulation, based on data recorded from Kartuzy WWTP.

The simulation conditions assume highly varying disturbances: Q, COD and TN, which are presented in the same order in Figs 10-12.

The performance, error and control signal trajectories of the closed loop system before and after the calibration process have been shown in Figs 13-18a).

Figs 13-18 indicate that the designed controller enables the system to realize the reference trajectory under the heavy time varying disturbances (Figs 10-12) keeping good performance over the whole operating range of the plant. It can be seen (Figs 15, 15a, 18, 18a) that both the magnitudes and rates of the demand control signal can be accommodated by the plant actuator system.

The control signal generated by not calibrated and calibrated systems are illustrated in Figs 15, 15a and 18, 18a, respectively. It can be seen that the control signals are equally demanding in terms of magnitudes and rates, however as it has been already stated the calibrated system achieves much better tracking error (see Table 4). The simulation was carried out under worst-case plant disturbance scenario (see Figs. 10 to 18).

As sample, the result of a daily performance, currently achieved by the control system, at the plant site, is illustrated in Fig. 19.

A significant improvement of operating performance by the proposed controller can be clearly seen.

Table 4. RMS and performance enhancement.

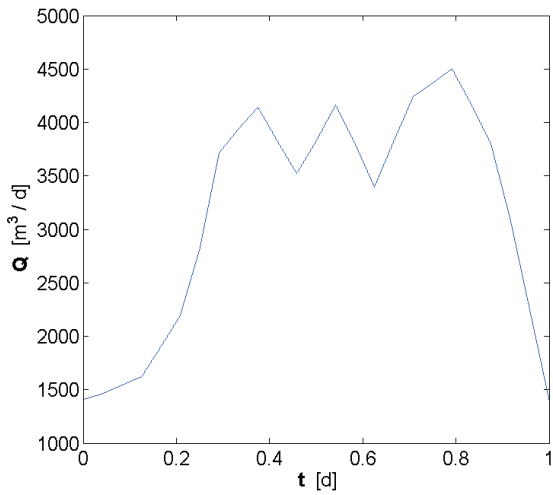| No	MF state	RMS	Percentage performance enhancement
1	before calibration	0,0218	0%
2	after calibration	0,0173	20,51%

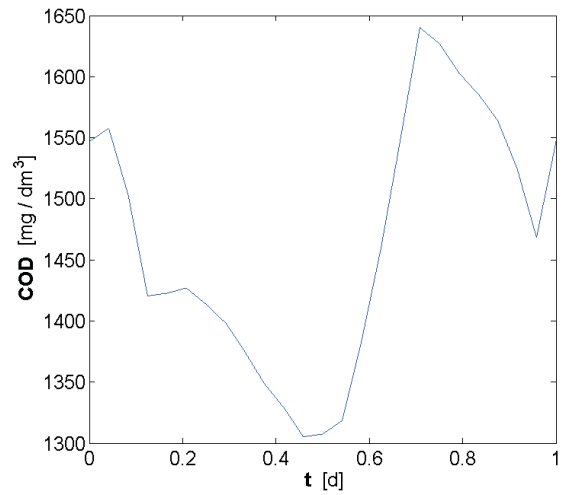Fig. 10. Inflow to WWTP.

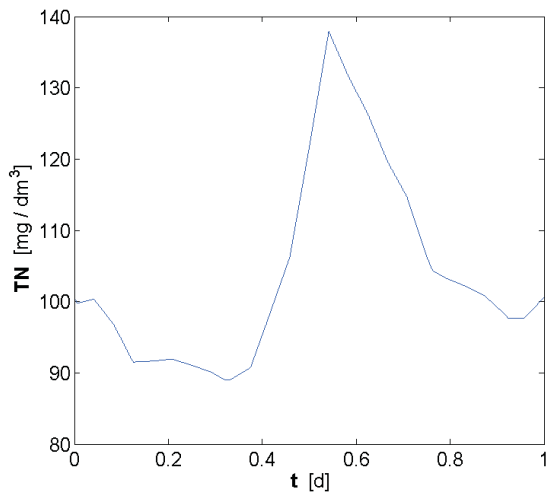Fig. 11. Chemical oxygen demand.
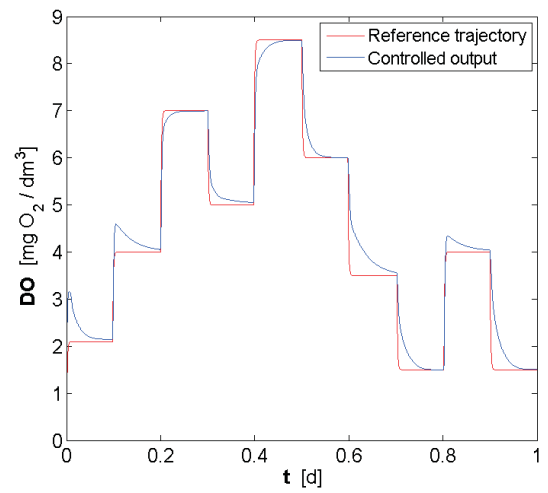

Fig. 12. Total nitrogen.

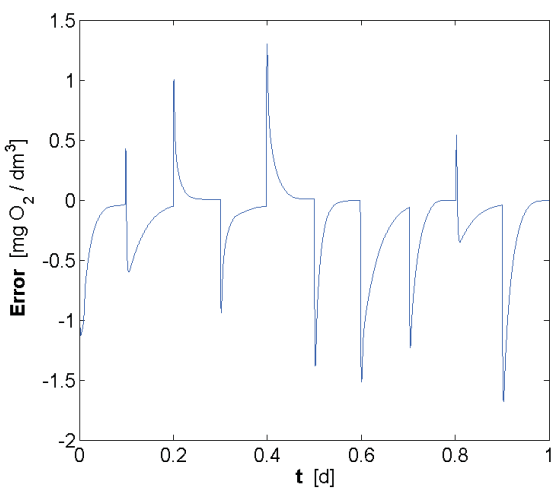Fig. 13. Closed loop system performance before calibration.
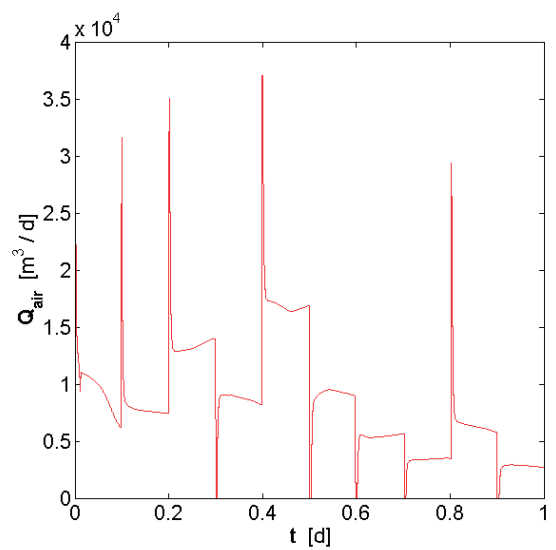

Fig. 14. Control error before calibration.

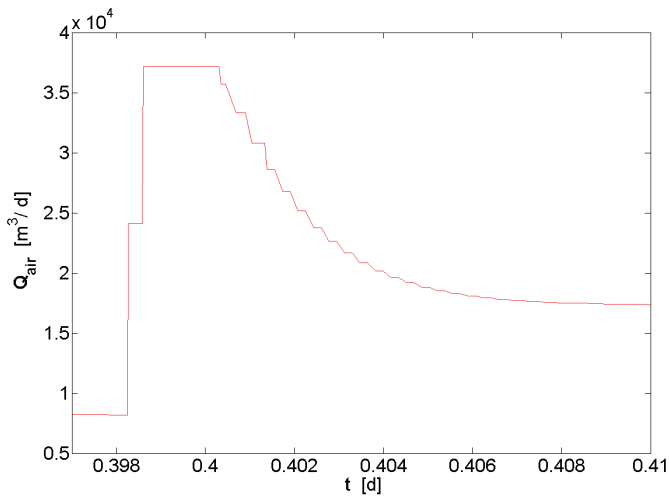Fig. 15. Controller output signal before calibration.

Fig. 15a. Zoom in of controller output - signal before calibration.
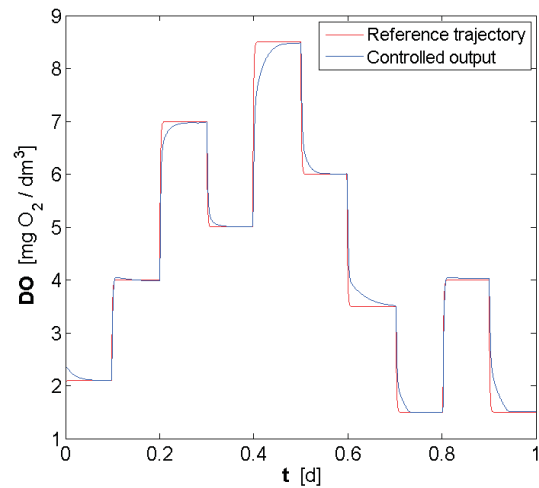

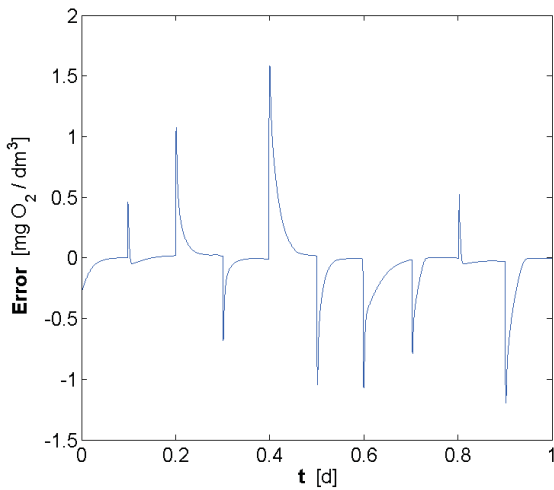Fig. 16. System performance after calibration.
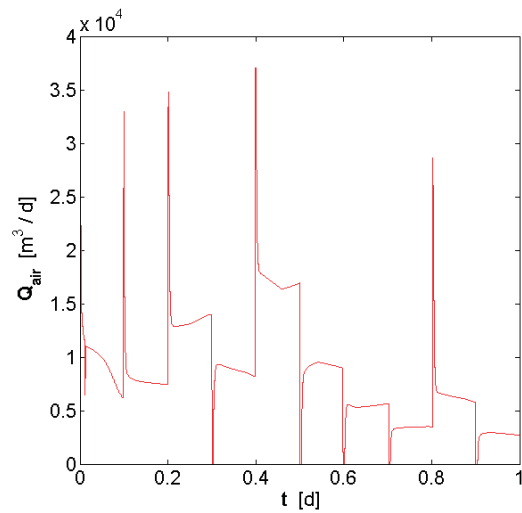

Fig. 17. Control error after calibration.

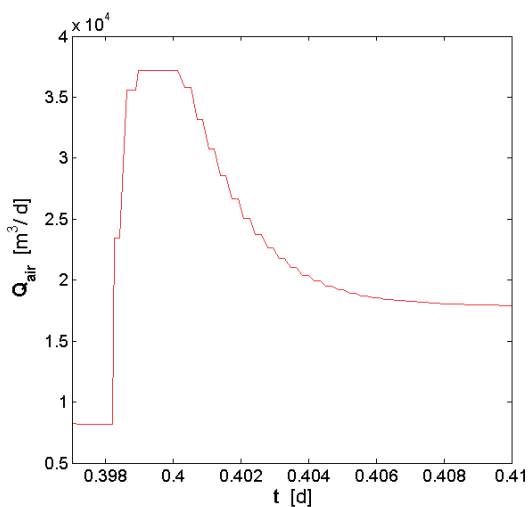Fig. 18. Controller output signal after calibration.

Fig. 18a. Zoom in of controller output - signal after calibration.

5. Conclusions

The paper has addressed design, calibration, implementation and simulation of the intelligent PI controller used for DO tracking in WWTP.

A classical PI controller has been used to derive multiregional intelligent controller. The controller is capable of maintaining globally well-known attractive local properties of the PI controller, when applied to nonlinear processes.

An advantageous property of the proposed controller design methodology is that it can be applied without changing the on plant (commonly used) hardware. Furthermore it allows obtaining great enhancement in the system performance via simple algorithm change, which is a low cost solution.

Enhancements are possible by calibrating MFs parameters.

The controller has been validated by simulation based on real data recorded from the Kartuzy WWTP and excellent results have been obtained, however a rigorous analysis of the closed loop stability is under current research.
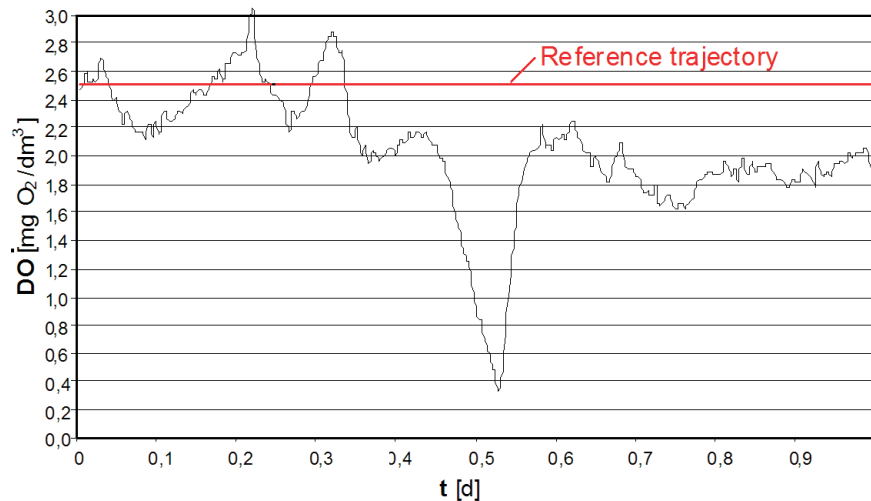
Fig. 19. Daily performance of the control systemat the plant site.

AUTHORS

Tomasz Zubowicz* - Department of Electrical Engineering and Automation, Gdansk University of Technology, 80-233 Gdansk, Poland. E-mail: tomasz.zubowicz@gmail.com.

Mieczysław A. Brdys - Gdansk University of Technology, Department of Electrical Engineering and Automation, 80-233 Gdansk, Poland. E-mail: m.brdys@ely.pg.gda.pl. Department of Electronic, Electrical and Computer Engineering, The University of Birmingham, Birmingham B15 2TT, UK. E-mail: m.brdys@bham.ac.uk.

Robert Piotrowski - Department of Electrical Engineering and Automation, Gdansk University of Technology, 80-233 Gdansk, Poland. E-mail: r.piotrowski@ely.pg.gda.pl.

* Corresponding author

References

[1]   Bohn C., Atherton D.P., An analysis package comparing PID anti - windup strategies. *Dept. of Electr. Eng.*, Ruhr-Univ., Bochum, 1995.

[2]   Brdys M.A., Chang T., Konarczak K., "Estimation of wastewater treatment plant state for model predictive control of N-P removal at medium time scale". In: *IFAC 10th Symposium Large Scale Systems: Theory and Applications*, Osaka, 26th-28th July 2004. (invite session).

[3]   Brdys M.A., Chotkowski W., Duzinkiewicz K., Konarczak K., Piotrowski R., "Two-level dissolved oxygen control for activated sludge processes". In: *15th IFAC World Congress*, Barcelona, 21st-26th July 2002.

[4]   Domanski P., Brdys M.A., Tatjewski P., "Design and stability of fuzzy logic multi - regional output controllers", *Int. Appl. Math. And Comp. Sci.*, vol. 9, no. 4, 1999, pp. 883-897.

[5]   Haupt R.L., Haupt S.E., *Practical Genetic Algorithms. Second Edition*. Wiley-Interscience, New Jersey, 2004.

[6]   Henze M., Gujer W., Mino W., Matsuo T., Wentzel M.C., Marais G.v.R., *Activated Sludge Model No. 2*. Scientific and Technical Report No. 3, IAWQ, London, 1995.

[7]   O'Reilly U-M., Yu T., Riolo R., Worze B., *Genetic Programing Theory and Practice II*. Springer Science, Boston, 2005.

[8]   Piotrowski R., Duzinkiewicz K., Brdys M.A, "Dissolved oxygen tracking and control of blowers at fast time scale". In: *IFAC 10th Symposium Large Scale Systems: Theory and Applications*, Osaka, 26th-28th July 2004.

[9]   Piotrowski R., Brdys M.A., Konarczak K., Duzinkiewicz K., Chotkowski W., "Hierarchical dissolved oxygen control for activated sludge processes", *Control Engineering Practice*, vol. 16, issue 1, 2008, pp. 114-131.

[10]   Simba, User's guide, 2005. http://simba.ifak.eu/simba.

[11]   Tanaka K., Sugeno M., "Stability analysis and designer of fuzzy control systems", *Fuzzy Sets Syst.*, vol. 45, 1992, pp. 135-166.

[12]   Yaochu Jin, *Advanced Fuzzy Systems Design and Applications*. Physica - Verlag. Springer - Verlag Company, 2002.

[13]   Yoo C.K., Lee H.K., Beum Lee I., "Comparison of process identification methods and supervisory control in the full scale wastewater treatment plant". In: *15th IFAC World Congress*, Barcelona, 21st-26th July 2002.